

Inelastic pion scattering from ^{13}C at 162 MeV

S. J. Seestrom-Morris*

*University of Minnesota, Minneapolis, Minnesota 55455
and Los Alamos National Laboratory, Los Alamos, New Mexico 87545*D. Dehnhard, M. A. Franey, and G. S. Kyle[†]*University of Minnesota, Minneapolis, Minnesota 55455*C. L. Morris, R. L. Boudrie, J. Piffaretti,[‡] and H. A. Thiessen*Los Alamos National Laboratory, Los Alamos, New Mexico 87545*

(Received 31 December 1981)

Differential cross sections for $^{13}\text{C}(\pi^{\pm}, \pi^{\pm'})^{13}\text{C}^*$ were measured at an incident pion energy of 162 MeV. Data were obtained for states or groups of states up to 21.6 MeV in excitation energy. The experimental results are compared with the distorted-wave impulse approximation calculations of Lee and Kurath.

<p>NUCLEAR REACTIONS $^{13}\text{C}(\pi^{\pm}, \pi^{\pm'})$, $T_{\pi}=162$ MeV; measured $\sigma(\theta)$. ^{13}C levels, deduced L_{π}. Comparison with microscopic DWIA calculation.</p>
--

I. INTRODUCTION

Inelastic pion scattering provides perhaps the most sensitive method to extract the relative contributions of neutron and proton particle-hole excitations to inelastic scattering. At pion energies near 180 MeV, the pion-nucleus scattering process is dominated by the [3,3] resonance ($J = \frac{3}{2}$, $T = \frac{3}{2}$) in the pion-nucleon interaction. For [3,3] resonance dominance, the isospin properties of the pion-nucleon system result in the cross section for π^+p (π^-n) elastic scattering being nine times that for π^-p (π^+n) elastic scattering. If pion-nucleus scattering can be described in terms of the amplitudes for pion-nucleon scattering by use of an impulse approximation, this 9:1 enhancement should also be observed in pion-nucleus inelastic scattering. Transitions which proceed purely through proton (neutron) particle-hole excitations should be nine times stronger in π^+ (π^-) scattering than in π^- (π^+) scattering. In general, nuclear excitations involve both protons and neutrons, resulting in cross section ratios considerably different from 9. Thus stringent tests of the proton and neutron components of model wave functions should be possible if the impulse approximation is valid. Calculations using the distorted-wave impulse approximation (DWIA) and transition densities derived from shell model wave functions^{1,2} or from electron scattering

measurements^{3,4} have generally been successful in describing (π, π') data on p - and sd -shell nuclei.

Previously we reported briefly⁵ on the first observation of a ratio $\sigma(\pi^-)/\sigma(\pi^+)$ consistent with the value of 9 predicted by the impulse approximation for a pure neutron transition. This paper describes in some detail our study of the nucleus ^{13}C by measurement of inelastic pion scattering at 162 MeV. We present angular distributions for the collectively enhanced transitions to the states at 3.68 MeV ($\frac{3}{2}^-$) and 7.55 MeV ($\frac{5}{2}^-$), as well as for the transitions to states at 3.09 ($\frac{1}{2}^+$), 3.85 ($\frac{5}{2}^+$), 8.86 ($\frac{1}{2}^-$), and 9.50 ($\frac{9}{2}^+$) MeV, which are candidates for simple particle-hole excitations with respect to the target ground state. We also show angular distributions for groups of states seen at 16.05, 17.92, 21.37, and 21.60 MeV that appear to contain $\frac{7}{2}^+$ and/or $\frac{9}{2}^+$ states. The data for most of these states are compared with the microscopic DWIA calculations of Lee and Kurath.^{2,6} A strong transition to a group of states at 11.82 MeV is found to be consistent with an octupole excitation of a $\frac{5}{2}^+, \frac{7}{2}^+$ doublet predicted⁷ at about 12 MeV.

II. EXPERIMENTAL PROCEDURE

The data were taken using the energetic pion channel and spectrometer (EPICS) at the Clinton P.

Anderson Meson Physics Facility (LAMPF). The EPICS channel, consisting of four dipole magnets, three multipole focusing magnets, and four adjustable collimating jaws, provides a dispersed beam of dimensions 20 by 8 cm on the scattering target.⁸ The EPICS spectrometer consists of a quadrupole triplet and two dipole magnets. Particle trajectories are measured before and after the spectrometer by sets of multiwire proportional chambers. The particle trajectory information, along with the magnetic fields in the bending magnets, is used to calculate the excitation energy of the residual nucleus or, equivalently, the "missing mass."

An excitation energy spectrum from $^{13}\text{C} + \pi^-$ scattering at $\theta_{\text{lab}} = 62^\circ$ and $T_\pi = 162$ MeV is shown in Fig. 1. The target was a sheet of carbon, enriched in ^{13}C (99%), of dimensions 22.5×15 cm, areal thickness 209 mg/cm², and covered on both sides by thin Kapton foils (≈ 1 mg/cm²). Angular distributions were obtained between 20° and 106° in 3° steps. The reaction yields were extracted from the spectra by use of the line shape oriented fitting program LOAF.⁹ This program uses as a line shape a reference peak that can be specified from the data. A reference shape derived from the elastic peak in a π^+ spectrum at 62° was used in the fitting of all states below 11 MeV of excitation. Levels above the 10.6-MeV threshold for α -particle emission have non-negligible natural widths and therefore another reference shape was extracted from the peak at 11.82 MeV. The width of this peak appeared representative of the experimental line shapes for the higher-lying states and, therefore, was used to extract areas for the peaks at 11.82, 16.05, 17.92, 21.37, and 21.60 MeV.

The elastic group and the states in ^{13}C at 3.09, 3.68, and 3.85 MeV and ^{12}C at 4.44 MeV were fit-

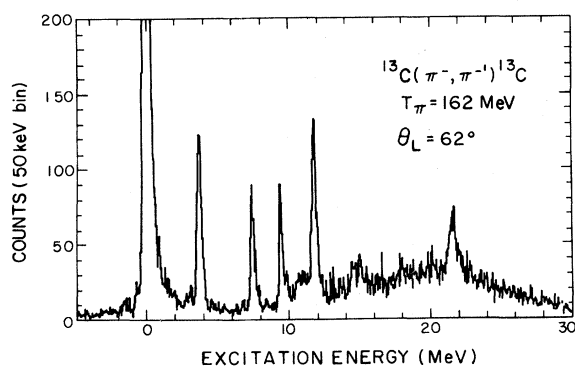


FIG. 1. A π^- spectrum taken at $\Theta_L = 62^\circ$ and $T_\pi = 162$ MeV. The energy resolution width (FWHM) is about 300 keV.

ted together, with the peak separations constrained by the tabulated energies of the states.¹⁰ The 3.68- and 3.85-MeV states were not resolved experimentally, as seen in Fig. 1, but the 3.68/3.85-MeV peak showed a larger width than other, single-state, peaks below 10.6 MeV. The attempt to extract separate areas for the two states seemed to be successful, but the area obtained for the weaker of the two, the 3.85-MeV state, was very sensitive to the width of the reference peak. The error in the extracted yield for this state due to the uncertainties in peak fitting is estimated to be $\approx 20\%$. A typical fit for this region is shown in Fig. 2.

Areas for the groups at 7.55, 8.86, 9.50, and 9.90 MeV were extracted simultaneously, with the separation between them constrained as mentioned above. All the groups above 10 MeV were fitted as "free" peaks, i.e., their separations were allowed to vary for the best fit. Their excitation energies were determined from the mean value of the centroids obtained at all angles. The structure of the group seen near 15 MeV changed as a function of angle and is probably due to transitions of several multiplicities, including the one to the weakly excited $T = \frac{3}{2}, J^\pi = \frac{3}{2}^-$ state at 15.1 MeV. Angular distributions for this group are not presented because of considerable problems in extracting the yields. (Rough estimates for the cross section of this group at a few angles may be obtained from the authors upon request.)

Yields were calculated relative to the charge collected in an ion chamber located behind the scattering target at 0° to the incident beam. The beam contained pions, protons, muons, and electrons. An absorber was placed before the ion chamber to stop any protons. The ion chambers thus detected only the energy losses of pions, muons, and electrons.

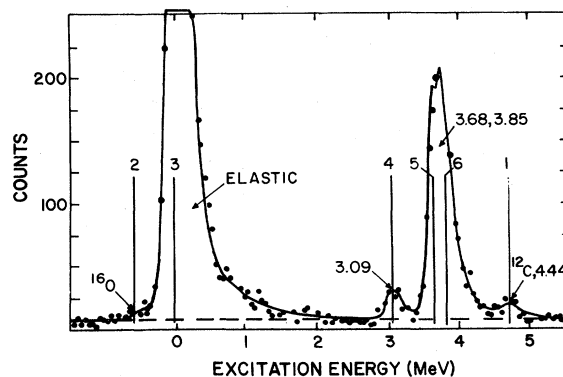


FIG. 2. Typical fit to the 0 to 5 MeV region in ^{13}C . The positions of the six peaks included in the fit are indicated.

The fractions of pions, muons, and electrons in the beam were measured by the time of flight method and used to determine the ion chamber response to pions. The yields were corrected for computer live time, chamber efficiencies, and pion decays in the spectrometer.¹¹ Furthermore, because the spectrometer acceptance is not constant over the entire momentum bite, an acceptance curve was obtained by measuring the yield for elastic scattering from ^{12}C at a fixed incident energy as a function of the spectrometer magnetic field. By varying the magnetic field, the elastic group was moved in steps from one edge of the spectrometer momentum bite to the other. The spectrum shown in Fig. 1 is not corrected for this variation in spectrometer acceptance. Thus the falloff in the yield from $E_x = 22$ to 30 MeV is due to the decrease in the spectrometer acceptance. Of course, all differential cross sections were properly corrected for this effect.

Absolute normalizations were determined relative to $\pi^\pm + ^{12}\text{C}$ elastic scattering cross sections previously measured with EPICS (Ref. 12) at LAMPF and at the Swiss Institute for Nuclear Research (SIN).¹³ (The two data sets are in agreement.) For this reason, we also measured yields for elastic scattering of π^+ and π^- from the ^{12}C in a 228 mg/cm² natural graphite target at $\theta_L = 65^\circ$ and $T_\pi = 162$ MeV.

The error bars in the figures for the differential cross sections represent only the statistical and fitting errors. No error bars are shown when these errors are smaller than the point size. Additional errors include $\pm 5\%$ due to uncertainties in the background, $\pm 2\%$ statistical errors in the acceptance scan, a $\pm 3\%$ uncertainty in the survival fraction correction, a $\pm 3\%$ uncertainty in the chamber efficiencies, $\pm 3\%$ in beam monitoring, and $\pm 5\%$ in the normalization to ^{12}C . Adding these errors in quadrature yields an overall error of $\pm 9\%$ in the absolute normalization. Some of the errors must be identical for π^+ and π^- scattering, namely errors in focal plane acceptance and survival fraction. Therefore, the uncertainty in the relative normalizations of the π^+ and π^- cross sections is believed to be $\pm 8\%$. As already mentioned, for the 3.85-MeV state an additional 20% error needs to be added due to the uncertainties in the peak fitting.

III. RESULTS AND COMPARISON WITH THEORY

A. Experimental results

The experimental angular distributions for the inelastic scattering are shown in Figs. 4 and 6–9,

along with microscopic model calculations to be discussed below. (The elastic scattering data together with a collective model analysis of the strong, collectively enhanced transitions will be presented in a forthcoming publication.) A brief summary of the π^-/π^+ differences is presented in Fig. 3. This figure is a plot of the asymmetry

$$A = (\sigma_{\pi^-} - \sigma_{\pi^+}) / (\sigma_{\pi^-} + \sigma_{\pi^+})$$

as a function of excitation energy, where the σ_{π^+} and σ_{π^-} are the values at the maxima of the angular distributions. The largest value, $A = 0.83 \pm 0.10$, for the $\frac{9}{2}^+$ state at 9.50 MeV, agrees with that expected for a pure neutron transition, $A = +0.8$. For the “single-neutron” states¹⁴ at 3.09 MeV ($\frac{1}{2}^+$) and at 3.85 MeV ($\frac{5}{2}^+$) known from $^{12}\text{C}(d,p)$ values of $A = 0.26 \pm 0.10$ and $A = 0.30 \pm 0.10$, respectively, were obtained which are much smaller than the free $\pi+n$ value. The ($\frac{3}{2}^-$) (3.68 MeV) and ($\frac{5}{2}^-$) (7.55 MeV) states of the weak-coupling doublet

$$[^{12}\text{C}(2^+, T=0) \otimes \nu(1p_{1/2})]$$

have quite different asymmetries. For the $\frac{3}{2}^-$ state the asymmetry is consistent with zero but for the $\frac{5}{2}^-$ state it is $A = -0.26 \pm 0.03$, which implies that this transition involves more protons than neutrons. The $\frac{1}{2}^-$ state at 8.86 MeV also has a negative asymmetry, $A = -0.27 \pm 0.13$. There are a number of large asymmetries in the region between 15 and 22 MeV. A group at 16.05 MeV has a large negative asymmetry, $A = -0.5 \pm 0.2$, i.e., not far from the free $\pi+p$ value of -0.8 . In addition, there is a

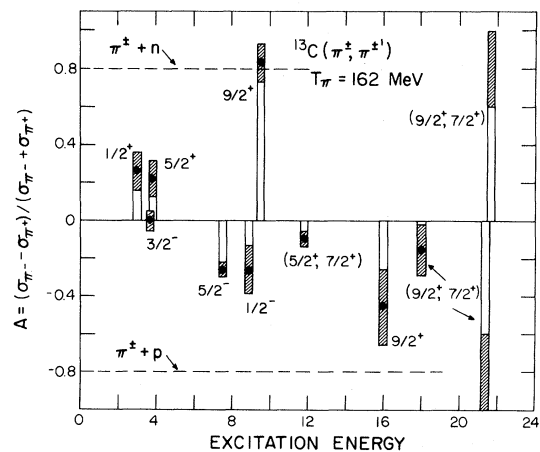


FIG. 3. Values of $A [=(\sigma_{\pi^-} - \sigma_{\pi^+}) / (\sigma_{\pi^-} + \sigma_{\pi^+})]$ for $^{13}\text{C}(\pi^\pm, \pi^\pm)$ extracted at the maxima of the differential cross sections, with crosshatching indicating the uncertainty in A .

group at about 21.5 MeV for which the centroid is lower in energy in π^+ than in π^- scattering. At 17.92 MeV there is a group with $A \approx 0$.

The asymmetry at the peak of the angular distributions is a very useful concept for qualitative discussions. Nevertheless, in the comparison with theory (Sec. III C) we will make use of the complete angular distributions for π^+ and π^- , since they clearly contain more information.

B. The microscopic DWIA calculations

The microscopic model calculations used in this work were done by Lee and Kurath (LK) at Argonne National Laboratory.^{2,6} Their method, described in detail in Ref. 2, uses a momentum space formulation of the DWIA and microscopic form factors derived from shell-model calculations.^{7,15} The pion-nucleus interaction potential is factored into two terms, one containing the nuclear transition form factors and the other the pion-nucleon interaction matrix elements. The pion-nucleon interaction matrix elements and the distorted waves are obtained from the momentum-space elastic scattering code, PIPIT.¹⁶

The shell-model states in ^{13}C may be divided into two groups, those of negative parity involving essentially only particles in the p shell and those of positive parity which involve at least one particle in the $2s1d$ shell or one hole in the $1s$ shell. In the LK calculations, the transition densities for the negative-parity states are obtained from the work of Cohen and Kurath (CK) (Ref. 15) in which only the excitations of particles within the $1p$ shell are considered. This model does not reproduce the collective quadrupole strength seen in ^{12}C and therefore the $\Delta J=2$, $\Delta L=2$, and $\Delta S=0$ transition density amplitudes are multiplied by enhancement factors like those needed to reproduce the measured $B(E2)$ values. Here ΔJ , ΔL , and ΔS are the total angular momentum, the orbital angular momentum, and the spin transfer, respectively, to the nucleus. Enhancement factors of 2.1 for neutrons and 1.4 for protons are used² for ^{13}C . The transition densities for the positive-parity states are obtained⁶ using wave functions based on a calculation of Millener and Kurath (MK).⁷ These wave functions are generated from a basis allowing (a) three particles in the $1s$ shell and ten particles in the $1p$ shell $[(1s)^3(1p)^{10}]$ or (b) four particles on the $1s$ shell, eight particles in the $1p$ shell, and one particle in the $2s1d$ shell $[(1s)^4(1p)^8(2s1d)^1]$. The effective interaction of Ref. 7 was modified by the authors of Ref. 6 to

reproduce more exactly the low-lying energy levels of ^{13}C . In this model, some of the low-lying states of ^{13}C have large overlaps with states formed by coupling a $(2s1d)$ shell neutron to the low-lying $T=0$ states of ^{12}C . Such states are expected to show large π^- enhancements. In the DWIA calculations the transition densities for the $1s$ to $1p$ excitations were omitted.

C. Comparison of data with model predictions

1. Transition to the $\frac{9}{2}^+$ state at 9.50 MeV

The most striking result of the (π, π') work on ^{13}C has been the observation⁵ of the very large asymmetry, $A = +0.83 \pm 0.10$, for the transition to the state at 9.50 MeV. The experimental angular distributions for this strongly π^- enhanced state are shown in Fig. 4. The broad shape and back-angle peaking of the angular distributions indicate a large

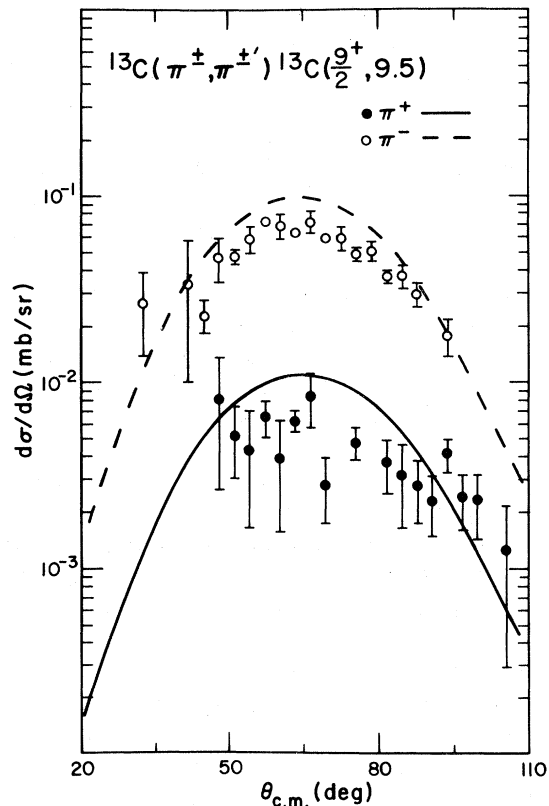


FIG. 4. Differential cross sections for (π^+, π^+) and (π^-, π^-) to the $\frac{9}{2}^+$ state at 9.50 MeV. Dashed (solid) lines are the LK calculations for π^- (π^+).

angular momentum transfer to a high-spin state. This suggestion is supported very strongly by the recent (e, e') work^{17,18} which revealed an almost pure $M4$ form factor for this transition.

This state can be identified with the first $\frac{9}{2}^+$ state predicted by Millener and Kurath.⁷ The identification of the lowest theoretical $\frac{9}{2}^+$ state with a state at 9.50 MeV was first suggested in Ref. 7 on the basis of three-particle transfer data.¹⁹ The DWIA calculations⁶ for this state reproduce the shape of the angular distributions very well (Fig. 4). The very large ratio

$$\sigma(\pi^-)/\sigma(\pi^+) \simeq 9 \quad (A = +0.83 \pm 0.10)$$

is also very well represented although the absolute magnitude of the calculations is larger than the data by about 20%. (The absolute experimental cross sections presented here are different from the preliminary results presented in Refs. 5 and 6 by a factor of about 0.8.)

The transition density predicted⁶ for this state is purely $\Delta J=4$, $\Delta L=3$, and $\Delta S=1$. This is the only allowed amplitude, as is clear from the following considerations. $J = \frac{9}{2}$ is the largest angular momentum that can be obtained by a particle-hole ($1p \rightarrow 2s1d$) excitation with respect to the ^{13}C ground state, i.e., the $\frac{9}{2}^+$ state is a "stretched" state. When a particle is promoted from a ($1p$) to a ($1d$) orbital, the orbital angular momentum transfers ΔL allowed are 1, 2, or 3. Since this transition is from a $\frac{1}{2}^-$ to a $\frac{9}{2}^+$ state, a total angular momentum transfer ΔJ of at least 4 is required. This can only be achieved by a spin transfer $\Delta S=1$. Thus the transition to the $\frac{9}{2}^+$ state is a pure "unnatural parity" transition [with $(-1)^{\Delta J} \neq (-1)^{\Delta L}$ and $\Delta S=1$ only] unlike most transitions in odd-mass nuclei to lower values of J which may proceed with a combination of $\Delta S=0$ and $\Delta S=1$.

It should be mentioned that the pure neutron character of the transition to the $\frac{9}{2}^+$ level can also be explained⁵ in terms of a simple weak-coupling model. When a $1d_{5/2}$ neutron is coupled to the first excited 2^+ , $T=0$ state of ^{12}C a $\frac{9}{2}^+$ state can be formed and the diagram given in Fig. 5(a) would represent one important component in the wave function. Indeed, the overlap of the weak-coupling wave function with the microscopic model wave function is very large.²⁰ The term on the right can be reached from a major component in the ^{13}C ground state [Fig. 5(b)] by a one-step, single neutron excitation from the $1p_{3/2}$ to the $1d_{5/2}$ shell. The excitation of the other term from the component in the ^{13}C ground state shown in Fig. 5(b) requires a

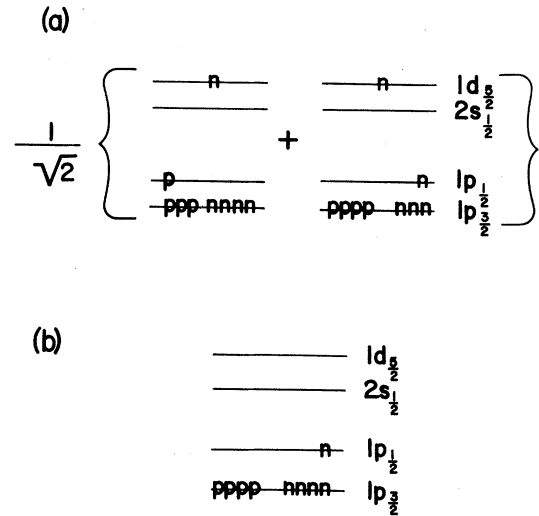


FIG. 5. Schematic shell model diagrams for (a) ^{13}C ($\frac{9}{2}^+$, 9.50 MeV) and (b) ^{13}C ground state.

two-step process; a proton must be promoted from the $1p_{3/2}$ to the $1p_{1/2}$ shell and a neutron from the $1p_{1/2}$ to the $1d_{5/2}$ shell. Therefore, under the assumption of a one-step direct reaction mechanism, such a state can only be reached by the promotion of a $1p_{3/2}$ neutron to the $1d_{5/2}$ shell.

In this model, states of $J^\pi = \frac{1}{2}^+$, $\frac{3}{2}^+$, $\frac{5}{2}^+$, and $\frac{7}{2}^+$ may also be formed by coupling a $1d_{5/2}$ neutron to ^{12}C (2^+ , $T=0$). However, an identification of these states with physical states is not simple because of strong mixing with other configurations, many of which could be reached by neutron and proton particle-hole excitations. However, the lowest lying "stretched" $\frac{9}{2}^+$ state can only be excited by moving a $1p_{3/2}$ neutron to the $1d_{5/2}$ shell. The transition to the $\frac{9}{2}^+$ member of the multiplet should therefore be more pure than those to the other members of the multiplet.

The weak-coupling model is also supported by the $^{12}\text{C}(n, n'\gamma)$ data²¹ which show preferential decay of the 9.50 MeV state to the 2^+ state in ^{12}C , and by the recent R -matrix analysis of Knox and Lane²² of $^{12}\text{C} + n$ scattering and reaction data.

2. Transitions to other high spin states

We find several transitions between 15 and 22 MeV that appear to be dominated by $\Delta J=4$, $\Delta L=3$, and $\Delta S=1$ components, since the angular distributions resemble the predicted curves for these angular momentum transfers (Figs. 6 and 7) and

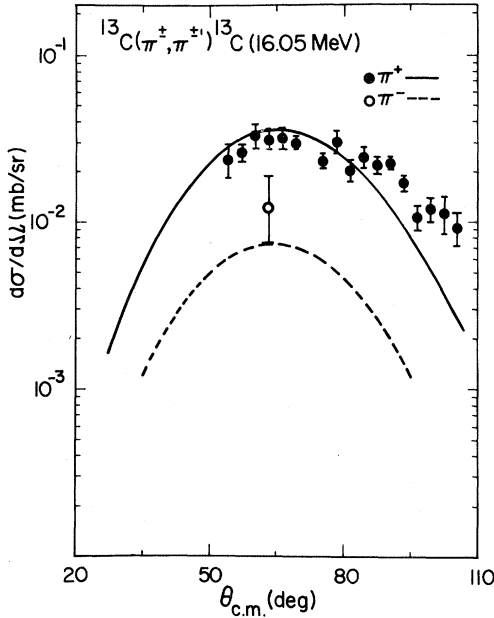


FIG. 6. Differential cross sections for (π^+, π^+) to the 16.05 MeV state in ^{13}C (solid circles) and the single point extracted for π^- (open circle). The solid (dashed) line is the result of the LK calculation for π^+ (π^-) to the third predicted $\frac{9}{2}^+$ state.

also the experimental angular distribution for the 9.50 MeV $\frac{9}{2}^+$ state. Excitation function measurements²³ have also indicated that these transitions are dominated by $\Delta S=1$. The centroids of these states are at 16.05 ± 0.05 , 17.92 ± 0.05 , 21.37 ± 0.05 , and 21.60 ± 0.05 MeV. The 16.05-MeV state is π^+ enhanced while the complex near 21.5 MeV peaks at 21.37 MeV in π^+ scattering and at 21.60 MeV in π^- scattering. The group at 17.92 MeV is about equally excited by π^+ and π^- .

A number of $\frac{7}{2}^+$ and $\frac{9}{2}^+$ states between 15 and 22 MeV are predicted⁶ to be dominated by the $\Delta J=4$, $\Delta L=3$, and $\Delta S=1$ amplitude. However, only for one case is it possible to make a fairly unambiguous identification with one of the predicted states, namely the state seen experimentally at 16.05 MeV. This state was indicated in the π^- spectra at several angles greater than 50° but we extracted a yield only from the best statistics spectrum at $\theta_L=62^\circ$. The calculations for the third predicted $\frac{9}{2}^+$ state are very close to the absolute magnitude of the π^+ data for the 16.05 MeV state (Fig. 6). The observed asymmetry $A = -0.5 \pm 0.1$ is in good agreement with the predicted value of $A = -0.6$.

The 21.5-MeV complex probably contains several

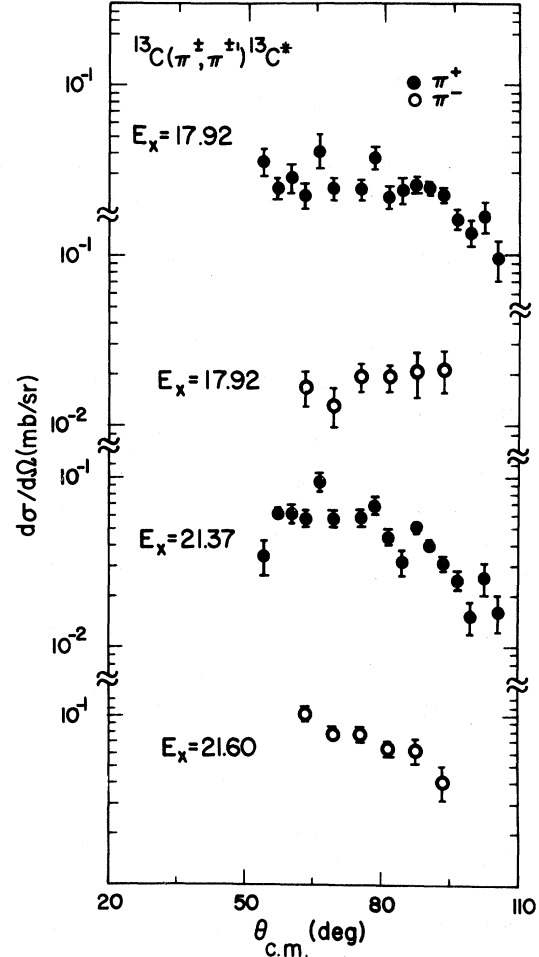


FIG. 7. Differential cross sections for (π^+, π^+) to states at 17.92 and 21.37 MeV in ^{13}C (solid circles) and for (π^-, π^-) to states at 17.92 and 21.60 MeV (open circles).

$\frac{7}{2}^+$ and $\frac{9}{2}^+$ states. None of the calculations⁶ for individual states around 21 MeV reproduce the magnitude of the cross sections or the $\sigma(\pi^+)/\sigma(\pi^-)$ ratio seen in the 21 MeV complex. However, the calculations do predict about equal π^+ and π^- strength and the total experimental π^- strength is about equal to the total experimental π^+ strength. Furthermore, the summed theoretical cross sections for states in this region are in qualitative agreement with the summed experimental cross sections.

However, the calculations do not predict the large π^-/π^+ asymmetries observed experimentally. This may be due to the fact that the calculations did not include the effects of isospin mixing. Evidence for strong isospin mixing has been deduced for two 4^- states at ≈ 19 MeV in ^{12}C from $^{12}\text{C}(\pi, \pi')$.²⁴ The

great similarity in the ^{13}C and $^{12}\text{C}(\pi, \pi')$ spectra in this energy region suggests that the high-spin states seen in ^{13}C close to 21 MeV are also isospin mixed like the 4^- states in ^{12}C .

The 180° electron scattering data^{17,18} are in agreement with our $\Delta J=4$, $\Delta S=1$ assignments for some of these transitions. The authors of Refs. 17 and 18 found $M4$ transitions to states at 9.49, 16.06, and 21.43 MeV but did not see any significant strength at ≈ 17.9 MeV. As we already pointed out in Ref. 23, a comparison of the different excitation strengths from the (π^+, π^+) , (π^-, π^-) , and (e, e') allows conclusions about the isospin transfer ΔT since the transverse (e, e') form factor is dominated by $\Delta T=1$. The near equality of $\sigma(\pi^-)$ and $\sigma(\pi^+)$ for the group at 17.92 MeV suggests a pure isospin transfer of either $\Delta T=0$ or $\Delta T=1$, but the lack of any significant $M4$ strength from (e, e') strongly supports a pure $\Delta T=0$ transition. The excitation energy of one of the strong $M4$'s from (e, e') , $E_x = 21.43 \pm 0.03$ MeV,¹⁸ is close to the centroid of the peak seen in (π^+, π^+) . This suggests a concentration of the $\Delta T=1$ strength in the lower energy part of the 21.5-MeV complex.

3. Transitions to the "single-particle" states at 3.09 MeV ($\frac{1}{2}^+$) and at 3.85 MeV ($\frac{5}{2}^+$)

The upper two sets of angular distributions, for (π^+, π^+) and (π^-, π^-) , presented in Fig. 8 are for the states at 3.09 MeV ($\frac{1}{2}^+$) and 3.85 MeV ($\frac{5}{2}^+$). The $\frac{1}{2}^+$ state is excited more strongly by π^- than by π^+ , with $R = \sigma(\pi^-)/\sigma(\pi^+) = 1.7 \pm 0.3$ or $A = +0.26 \pm 0.10$. In the simple shell model the wave function for this state is that of a $2s_{1/2}$ neutron coupled to the ^{12}C ground state. The results of the $^{12}\text{C}(d, p)^{13}\text{C}$ reaction¹⁴ imply that this state contains a large fraction of the $2s_{1/2}$ single-particle strength. Thus the $\frac{1}{2}^+$ state should be reached mainly by a neutron $1p_{1/2} \rightarrow 2s_{1/2}$ promotion with a ratio $\sigma(\pi^-)/\sigma(\pi^+)$ of about 9. However, the observed very small $\sigma(\pi^-)/\sigma(\pi^+)$ ratio indicates that this transition is not a pure neutron transition. Similarly, the comparison of $B(E1)$ values²⁵ for this state and its analog in ^{13}N yields a ratio of neutron to proton components that predicts $\sigma(\pi^-)/\sigma(\pi^+) = 1.6$, in agreement with our results.

In the shell model calculation of Ref. 7 the principal neutron character of the simple shell model prediction for this transition is largely retained, in contradiction to the π^+ data. The π^- angular distribution is reproduced reasonably well by the calcu-

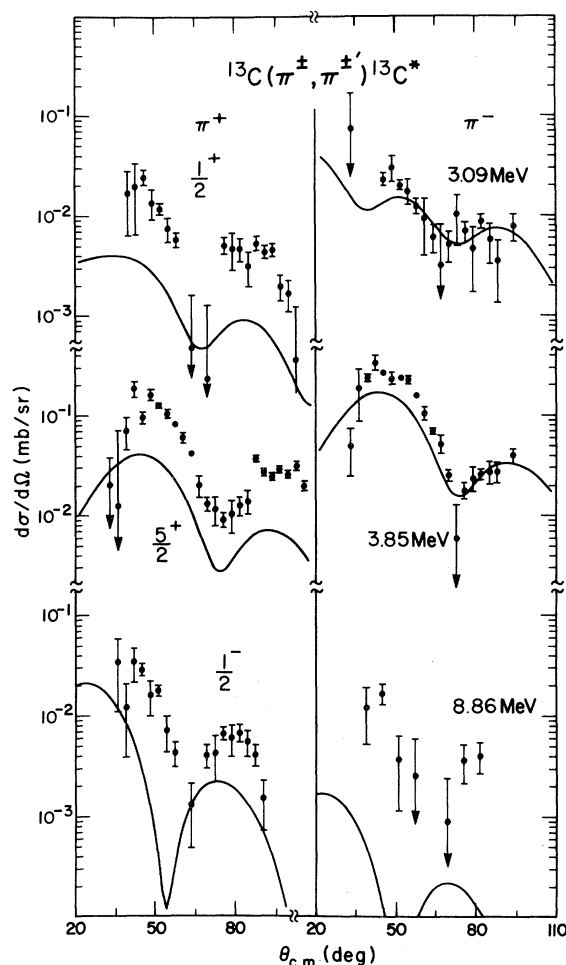


FIG. 8. Differential cross sections for (π^+, π^+) , on the left, and (π^-, π^-) , on the right, to the $\frac{1}{2}^+$ (top), $\frac{5}{2}^+$ (middle), and $\frac{1}{2}^-$ (bottom) states in ^{13}C . The solid curves are the LK calculations for these states.

lations,⁶ but the π^+ predictions are a factor of 6 smaller than the data. We note that although the uncertainties in the magnitude of the DWIA calculations are quite large, the uncertainties affect π^+ and π^- in a similar way. Thus, comparisons of the measured and predicted π^+/π^- ratios are at present more stringent tests of the wave functions and/or the reaction mechanism than are comparisons of experimental and theoretical absolute cross sections for either probe separately.

According to Ref. 6, the π^- transition is dominated by the $(\Delta L=1, \Delta S=0)$ transition density amplitudes, while for π^+ the $(\Delta L=1, \Delta S=0)$ and $(\Delta L=1, \Delta S=1)$ amplitudes are of comparable magnitude. The $(\Delta L=1, \Delta S=0)$ amplitude is inhibited for both π^+ and π^- by the destructive in-

interference between the amplitudes for $(1p) \rightarrow (1d)$ and $(1p) \rightarrow (2s)$ excitation. However, since most of the $(1p) \rightarrow (2s)$ amplitude is due to almost pure neutron excitation from the $1p_{1/2}$ shell to the $2s_{1/2}$ shell, the interference affects π^+ and π^- very differently, resulting in predictions of quite different shapes for the π^+ and π^- angular distributions. (Although the errors are quite large for these weak transitions, the experimental π^+ and π^- angular distributions indicate different shapes.)

The gross underestimation of the π^+ cross section suggests that the ground state of ^{13}C as described by the CK wave functions has too few protons in the $1p_{1/2}$ orbit. An increase in the ground state components that involve $1p_{1/2}$ protons could increase the proton $1p_{1/2}$ to $2s_{1/2}$ amplitude, decrease the $1p_{3/2}$ to $1d_{5/2}$ amplitude, and result in less destructive interference mainly for π^+ scattering so that the π^+ cross section would increase relative to the π^- cross section. Components in the ^{13}C ground state with two particles in the $(2s\ 1d)$ shell might also increase the cross section for exciting this state, and make the neutron and proton components of the transition density more equal.

The second set of angular distributions in Fig. 8 shows the π^+ and π^- data for the $\frac{5}{2}^+$ state at 3.85 MeV. This state is also strongly excited in $^{12}\text{C}(d,p)$ and it should contain a large fraction of the $1d_{5/2}$ single particle strength. However, the π^- cross section is larger than the π^+ cross section only by a factor of 2 ($A = +0.3 \pm 0.1$). The calculations⁶ successfully predict the positions of the maxima and minima in the angular distributions but the absolute magnitude is too low for both π^+ and for π^- . More significantly, the calculated ratio $\sigma(\pi^-)/\sigma(\pi^+)$ is 4.2 ($A = +0.62$), much larger than the experimental value. As for the $\frac{1}{2}^+$ state, the transition to this state appears not as neutron dominated as the MK calculations⁷ indicate.

4. Transition to the $\frac{1}{2}^-$ state at 8.86 MeV

The last set of angular distributions in Fig. 8 is for the $\frac{1}{2}^-$ state at 8.86 MeV. This state is of interest because of its very large overlap²⁰ with a $^{14}\text{C}(1^+) \otimes p_{1/2}^{-1}$ configuration which is predicted to be reached by a pure $\Delta S = 1$, pure proton excitation. The transition to this state is very weak and the error bars are quite large. The calculations fail to reproduce both the absolute cross sections and the π^+/π^- ratio. The predicted π^+/π^- ratio is about ten, but the experimental ratio is only be-

tween one and two. For π^+ the calculated angular distribution is shifted out of phase with respect to the data. The CK model¹⁵ predicts proton amplitudes much larger than the neutron amplitudes only for the dominant ($\Delta L = 0$, $\Delta S = 1$) amplitude.² For the other amplitudes the proton to neutron ratio is about two. Thus the data suggest that the relative importance of the ($\Delta L = 0$, $\Delta S = 1$) proton amplitude has been overestimated. In addition, the predicted transition density is purely $\Delta S = 1$, whereas excitation function measurements imply¹¹ that this is not the case. Of course, since the predicted transition density amplitudes are quite small the above discrepancies might be due to more complicated reaction mechanisms than assumed in Ref. 2.

5. Collectively enhanced $\Delta L = 2$ transitions to the $\frac{3}{2}^-$ (3.68 MeV) and $\frac{5}{2}^-$ (7.55 MeV) states

The data and calculations for the $\frac{3}{2}^-$ (3.68 MeV) and $\frac{5}{2}^-$ (7.55 MeV) states are shown in Fig. 9 (top and center). The π^+ and π^- cross sections to the $\frac{3}{2}^-$ state are approximately equal ($A = 0.00 \pm 0.05$), in good agreement with the DWIA predictions in which enhancement factors for the $\Delta L = 2$, $\Delta S = 0$ amplitudes are included. However, the calculated absolute cross sections are higher than the data near the maxima of the angular distributions, indicating the need for slightly smaller enhancement factors. The same enhancement factors were used for the $\frac{3}{2}^-$ and $\frac{5}{2}^-$ states.

The experimental cross sections for the $\frac{5}{2}^-$ state for (π^+, π^+') are larger than for (π^-, π^-') by a factor $R = \sigma(\pi^+)/\sigma(\pi^-) = 1.69 \pm 0.07$, i.e., $A = -0.26 \pm 0.03$. The LK calculations² predict a π^+ enhancement as well, i.e., $\sigma(\pi^+)/\sigma(\pi^-) = 2.6$. For π^- scattering there is a non-negligible contribution predicted from the experimentally unresolved $\frac{7}{2}^+$ state at 7.49 MeV [which contains a large component of the wave function of the $\frac{7}{2}^+$ member of the $(2^+ \times 1d_{5/2})$ weak-coupling multiplet]. The dotted-dashed lines give the LK results for the $\frac{7}{2}^+$ state, the dashed line for the $\frac{5}{2}^-$ state, and the solid line for the sum of the two. The contribution from the $\frac{7}{2}^+$ state is quite large near the minimum in the π^- angular distribution but it is barely visible for π^+ . Even when the effects of the $\frac{7}{2}^+$ state are included, the calculations predict a π^+ enhancement slightly larger than is observed experimentally.

In a weak-coupling model, the $\frac{3}{2}^-$ and $\frac{5}{2}^-$ states are often interpreted as states formed by coupling a

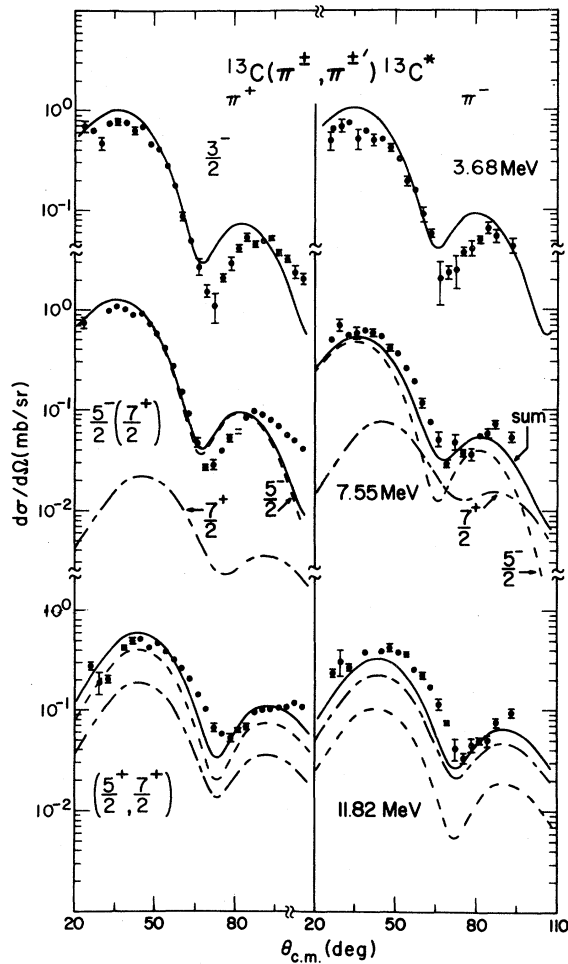


FIG. 9. Differential cross sections for (π^+, π^+) , on the left, and (π^-, π^-) , on the right, to the $\frac{3}{2}^-$ (top), $\frac{5}{2}^-$, $\frac{7}{2}^+$ (middle), and $\frac{5}{2}^+$, $\frac{7}{2}^+$ (bottom) states in ^{13}C . The solid curves with the $\frac{3}{2}^-$ state are the LK calculations for that state. The dashed curves with the $\frac{5}{2}^-$, $\frac{7}{2}^+$ doublet are the LK calculations for the $\frac{5}{2}^-$, the dotted-dashed curves are for the $\frac{7}{2}^+$, and the solid curve is the sum of the $\frac{5}{2}^-$ and $\frac{7}{2}^+$ predictions. The dashed curves for the proposed $\frac{5}{2}^+$, $\frac{7}{2}^+$ doublet are the LK calculations for the fourth predicted $\frac{5}{2}^+$, the dotted-dashed curves are for the second predicted $\frac{7}{2}^+$, and the solid curve is the sum.

$1p_{1/2}$ neutron to the collective 2^+ , $T=0$ state in ^{12}C , whereas the ground state (g.s.) of ^{13}C is obtained by coupling a $1p_{1/2}$ neutron to the ^{12}C g.s. Since the $0^+ \rightarrow 2^+$ transition in ^{12}C is isoscalar, equal π^+ and π^- cross sections would be expected in this simple model for the transitions to the $\frac{3}{2}^-$ and $\frac{5}{2}^-$ states in ^{13}C . The observed experimental and calculated theoretical π^+ enhancement of the $\frac{5}{2}^-$ state transition can be qualitatively understood

as a blocking effect in the following way.

A large component in the 2^+ -state wave function consists of equal parts neutron and proton $(1p_{3/2})^{-1}(1p_{1/2})$ particle-hole (p-h) excitation relative to the ^{12}C g.s. Simple two particle-one hole (2p-1h) states are formed when a $1p_{1/2}$ neutron is added to this part of the 2^+ -state wave function. The proton $[(1p_{3/2})^{-1}(1p_{1/2})]_{2+}$ terms can couple with the $1p_{1/2}$ neutron to either $J^\pi = \frac{3}{2}^-$ or $J^\pi = \frac{5}{2}^-$. However, the neutron $[(1p_{3/2})^{-1}(1p_{1/2})]_{2+}$ terms can only yield $J^\pi = \frac{3}{2}^-$ when coupled with the $1p_{1/2}$ neutron because the two $1p_{1/2}$ neutrons must couple to $J^\pi = 0^+$. Thus the spin of this configuration must equal the spin of the $1p_{3/2}$ hole. The former configuration can only be reached by proton p-h excitation from the ^{13}C g.s. and the latter can only be reached by neutron p-h excitation. Both configurations will contribute to the $\frac{3}{2}^-$ state but only the former (reached by proton p-h excitation) can contribute to the $\frac{5}{2}^-$ state. Of course, the physical states involve many other configurations in addition to the two just mentioned. Nevertheless, the blocking of the neutron p-h excitations is expected to be larger for the $\frac{5}{2}^-$ state than for the $\frac{3}{2}^-$ state. This is in agreement with the experimental asymmetries of $A = 0.26 \pm 0.03$ for the $\frac{5}{2}^-$ state and $A = 0.00 \pm 0.05$ for the $\frac{3}{2}^-$ state. This difference in the asymmetries for the $\frac{3}{2}^-$ and $\frac{5}{2}^-$ states is an example of a J -dependent blocking effect for the two states of a weak-coupling doublet.

6. Evidence for a $\Delta L = 3$ transition to a $\frac{7}{2}^+$, $\frac{5}{2}^+$ doublet (11.82 MeV)

The last set of curves in Fig. 9 presents the data for the group seen at 11.82 MeV. The cross sections for π^+ and π^- scattering are nearly equal, i.e., $A = -0.10 \pm 0.05$. The angular distributions peak at a larger angle than do the angular distributions for the $\frac{3}{2}^-$ and $\frac{5}{2}^-$ states. This indicates that the transition is dominated by an angular momentum transfer larger than $\Delta L = 2$. Apparently, the known $\frac{3}{2}^-$ state reported at this excitation energy¹⁰ is not excited appreciably but rather a state (or states) of higher spin, i.e., $\frac{5}{2}^+$ and/or $\frac{7}{2}^+$. Indeed, contributions from inelastic scattering to the known $\frac{3}{2}^-$ state are expected²⁰ to be very small.

Plotted with the data for the 11.82-MeV group are the theoretical $\Delta L = 3$ angular distributions⁶ for the second predicted $\frac{7}{2}^+$ state (dotted-dashed line) and the fourth predicted $\frac{5}{2}^+$ state (dashed line), both calculated to lie near 12 MeV and the strongest states predicted in the region. The summed theoret-

ical cross sections (solid lines) reproduce the shape and magnitude of the data quite well, although they are slightly below the π^- data and slightly above the π^+ data at their peaks. The calculations contain no enhancement factors for $\Delta L = 3$ type transitions and the wave functions^{6,20} for these states are not dominated by terms corresponding to a $1p_{1/2}$ neutron coupled to the collective 3^- state (9.64 MeV) in ^{12}C . The agreement with the data indicates that no enhancement is necessary, in contrast to the strongly enhanced $E3$ in ^{12}C .

The DWIA predictions for the $\frac{5}{2}^+$ state at 3.85 MeV (Sec. III C 3) are below the data for both π^+ and π^- . This lack of agreement might be due to mixing between that state and the $\frac{5}{2}^+$ state at about 12 MeV, with the $\frac{1}{2}^- \rightarrow \frac{5}{2}^+$ fraction of the octupole strength being split between them. Nonetheless, the total experimentally observed $\Delta L = 3$ cross section would not be quite reproduced in the calculations, thus indicating the need for a small enhancement of the $\Delta J = 3$, $\Delta L = 3$, and $\Delta S = 0$ amplitudes. In any case, it appears clear that the strongly collective $E3$ transition in ^{12}C has no equivalent in ^{13}C .

IV. SUMMARY AND CONCLUSIONS

This work comprises a study of the nucleus ^{13}C with inelastic pion scattering. High resolution (π^+, π^+) and (π^-, π^-) data were taken using the EPICS facility at the Clinton P. Anderson Meson Physics Facility. Differential cross sections were measured for angles between 20° and 105° at an incident pion energy of 162 MeV. The experimental angular distributions have been compared with the DWIA calculations of Lee and Kurath. The predicted angular distributions are generally successful in reproducing the shapes of the experimental angular distributions but in many cases fail to reproduce the magnitude of the cross sections.

For a pure neutron particle-hole transition predicted by shell-model calculations for the $\frac{9}{2}^+$ state at 9.50 MeV the experimental asymmetry is reproduced within errors but the magnitudes of the predicted cross sections are larger than the data. This discrepancy in absolute magnitude needs further study, especially in light of the recent results on quenching of magnetic transitions which showed even larger disagreement with simple model predictions.²⁶ Indeed, we have done preliminary DWIA calculations with different optical potentials that yield larger theoretical cross sections for the $\frac{9}{2}^+$ state than presented here.⁶ The predicted cross section ratio $\sigma(\pi^-)/\sigma(\pi^+)$ is still close to nine, howev-

er, independent of the details of the calculation. The pure neutron particle-hole character of this transition should provide a good test case for future detailed comparison of pion, proton, and electron scattering.

Four states between 15 and 22 MeV have been identified as high-spin states. The angular distributions are characteristic of those predicted for transitions dominated by $\Delta J = 4$, $\Delta L = 3$, and $\Delta S = 1$. One of these states, at 16.05 MeV, has been identified with the third predicted $\frac{9}{2}^+$ state of Millener and Kurath. The π^-/π^+ asymmetry seen near 21.5 MeV suggests that there is isospin mixing between $T = \frac{1}{2}$ and $T = \frac{3}{2}$ states of spin, parity $J^\pi = \frac{7}{2}^+$ and/or $\frac{9}{2}^+$.

The DWIA calculations of Lee and Kurath with enhancement factors for the $\Delta J = 2$, $\Delta L = 2$, and $\Delta S = 0$ amplitudes determined from electromagnetic measurements reproduce reasonably well the shapes and the magnitude of the cross sections for the collectively enhanced transitions to the $\frac{3}{2}^-$ (3.68) and $\frac{5}{2}^-$ (7.55) states.

Evidence was found for a $\Delta L = 3$ transition to a $\frac{7}{2}^+, \frac{5}{2}^+$ doublet at 11.82 MeV.

Large discrepancies were observed between theory and experiment for the "single-particle" transitions and the transition to the $\frac{1}{2}^-$ state at 8.86 MeV. In each of these cases larger π^+/π^- asymmetries were predicted than were measured, since the weaker transition was considerably stronger than predicted. Because these transitions are extremely weak the discrepancies are probably, at least in part, due to more complicated reaction mechanisms, such as two-step processes. Although we are aware of this possibility, we have discussed in some detail alternative explanations arising from possible problems in the nuclear structure predictions.

It is clear from both our successes and failures in comparing our (π, π') data with DWIA calculations using shell model predictions that further theoretical analysis of these data is worthwhile. Especially useful will be a consistent analysis of the same transitions induced by different but complementary probes.

ACKNOWLEDGMENTS

We thank Dr. D. Kurath, Dr. T.-S. H. Lee, Dr. B. Bayman, and Dr. P. Ellis for many helpful discussions. We are especially grateful to Dr. T.-S. H. Lee and Dr. D. Kurath for making their DWIA calculations available to us before publication. This work was supported in part by the United States Department of Energy.

- *Present address: Los Alamos National Laboratory, Los Alamos, NM 87544.
- †Present address: Schweizerisches Institut für Nuklearforschung, CH-5234 Villigen, Switzerland.
- ‡Present address: Institute de Physique, Université de Neuchâtel, CH-2000 Neuchâtel, Switzerland.
- ¹T.-S. H. Lee and R. D. Lawson, *Phys. Rev. C* **21**, 679 (1980).
- ²T.-S. H. Lee and D. Kurath, *Phys. Rev. C* **21**, 293 (1980).
- ³L. Morris, K. G. Boyer, C. Fred Moore, C. J. Harvey, K. J. Kallianpur, I. B. Moore, P. A. Seidl, S. J. Seestrom-Morris, D. B. Holtkamp, S. J. Greene, and W. B. Cottingame, *Phys. Rev. C* **24**, 231 (1981).
- ⁴K. G. Boyer, W. B. Cottingame, L. E. Smith, S. J. Greene, C. Fred Moore, J. S. McCarthy, R. C. Minehart, J. F. Davis, G. R. Bureson, G. Blanpied, C. A. Goulding, H. A. Thiessen, and C. L. Morris, *Phys. Rev. C* **24**, 598 (1981).
- ⁵D. Dehnhard, S. J. Tripp, M. A. Franey, G. S. Kyle, C. L. Morris, R. L. Boudrie, J. Piffaretti, and H. A. Thiessen, *Phys. Rev. Lett.* **43**, 1091 (1979).
- ⁶T.-S. H. Lee and D. Kurath, *Phys. Rev. C* **22**, 1670 (1980).
- ⁷D. J. Millener and D. Kurath, *Nucl. Phys.* **A255**, 315 (1975).
- ⁸H. A. Thiessen and S. Sobottka, Los Alamos Scientific Laboratory Report No. LA-4534-MS, 1970.
- ⁹Lester Eugene Smith (unpublished).
- ¹⁰F. Ajzenberg-Selove, *Nucl. Phys.* **A152**, 1 (1970).
- ¹¹S. J. Seestrom-Morris, Ph.D. dissertation, University of Minnesota, 1981.
- ¹²K. G. Boyer, private communication.
- ¹³J. Piffaretti, R. Corfu, J.-P. Egger, P. Gretillat, C. Lunke, E. Schwarz, C. Perrin, and B. M. Preedom, *Phys. Lett.* **71B**, 324 (1977); private communication.
- ¹⁴S. E. Darden, S. Sen, H. R. Hiddleston, J. A. Aymar, and W. A. Yoh, *Nucl. Phys.* **A208**, 77 (1973).
- ¹⁵S. Cohen and D. Kurath, *Nucl. Phys.* **73**, 1 (1965).
- ¹⁶R. A. Eisenstein and F. Tabakin, *Comput. Phys. Commun.* **12**, 237 (1976).
- ¹⁷R. S. Hicks *et al.*, Proceedings of the Workshop on Nuclear Structure with Intermediate Energy Probes, Los Alamos, edited by H. A. Thiessen, Los Alamos Scientific Laboratory Report LA-8303-C, 1980, p. 292; J. Dubach *et al.* (unpublished).
- ¹⁸D. I. Sober, private communication.
- ¹⁹C. H. Holbrow, H. G. Bingham, R. Middleton, and J. D. Garrett, *Phys. Rev. C* **2**, 902 (1974).
- ²⁰D. Kurath, private communication.
- ²¹H. E. Hall and T. W. Bonner, *Nucl. Phys.* **14**, 295 (1959).
- ²²H. D. Knox and R. O. Lane, *Nucl. Phys.* **A378**, 503 (1982).
- ²³S. J. Seestrom-Morris, D. Dehnhard, D. B. Holtkamp, and C. L. Morris, *Phys. Rev. Lett.* **46**, 1447 (1981).
- ²⁴C. L. Morris, J. Piffaretti, H. A. Thiessen, W. B. Cottingame, W. J. Braithwaite, R. J. Joseph, I. B. Moore, D. B. Holtkamp, C. J. Harvey, S. J. Greene, C. Fred Moore, R. L. Boudrie, and R. J. Peterson, *Phys. Lett.* **86B**, 31 (1979).
- ²⁵P. Endt, *At. Data Nucl. Data Tables* **23**, 3 (1979).
- ²⁶A. Bohr and B. R. Mottelson, *Phys. Lett.* **100B**, 10 (1981).